

## Tumorigenesis and Neoplastic Progression

# The Role of *BRAF* Mutation and p53 Inactivation during Transformation of a Subpopulation of Primary Human Melanocytes

Hong Yu,\* Ronan McDaid,<sup>†</sup> John Lee,<sup>†</sup>  
Patricia Possik,<sup>†</sup> Ling Li,<sup>†</sup> Suresh M. Kumar,\*  
David E. Elder,\* Patricia Van Belle,\*  
Phyllis Gimotty,<sup>‡</sup> Matt Guerra,<sup>‡</sup>  
Rachel Hammond,<sup>‡</sup> Katharine L. Nathanson,<sup>§</sup>  
Maria Dalla Palma,<sup>§</sup> Meenhard Herlyn,<sup>†</sup>  
and Xiaowei Xu\*

From the Departments of Pathology and Laboratory Medicine,\*  
Biostatistics and Epidemiology,<sup>‡</sup> and Medicine,<sup>§</sup> University of  
Pennsylvania School of Medicine, Philadelphia, Pennsylvania;  
and The Wistar Institute,<sup>†</sup> Philadelphia, Pennsylvania

**Melanocytic nevi frequently harbor oncogenic *BRAF* mutations, but only a minority progress to melanoma. In human melanocytes, persistent *BRAF*<sup>V600E</sup> expression triggers oncogene-induced senescence, which implies that bypass of oncogene-induced senescence is necessary for malignant transformation of melanocytes. We show that a subpopulation of primary human melanocytes with persistent expression of *BRAF*<sup>V600E</sup> do not enter oncogene-induced senescence, but instead survive despite heightened MAPK activity. Disruption of the p53 pathway using short-hairpin RNA initiated rapid growth of these V600E<sup>+</sup> melanocytes *in vitro*. The resultant V600E<sup>+</sup>/p53<sup>sh</sup> melanocytes grew anchorage-independently in soft agar, formed pigmented lesions reminiscent of *in situ* melanoma in artificial skin reconstructs, and were weakly tumorigenic *in vivo*. Array comparative genomic hybridization analysis demonstrated that the transformed melanocytes acquired a substantial deletion in chromosome 13, which encodes the *Rb1* tumor suppressor gene. Gene expression profiling study of nevi and melanomas showed that p53 target genes were differentially expressed in melanomas compared with nevi, suggesting a dysfunctional p53 pathway in melanoma *in vivo*. In summary, these data demonstrate that a subpopulation of melanocytes possesses the ability to survive *BRAF*<sup>V600E</sup>-induced senescence, and suggest that p53 inactivation may promote malignant transforma-**

**tion of these cells.** (*Am J Pathol* 2009, 174:2367–2377; DOI: 10.2353/ajpath.2009.081057)

Melanocytic nevi (moles) are common benign human tumors. Eighty percent of nevi harbor *BRAF* mutations, with the most frequent mutation being a valine-to-glutamic acid substitution at position 600 (V600E).<sup>1</sup> *BRAF*<sup>V600E</sup> has highly-elevated kinase activity and confers constitutive activation of the MAPK pathway.<sup>2</sup> Although *BRAF* mutations are thought to be an early and critical step in the initiation of melanocytic neoplasia, the exact role of mutant *BRAF* in human melanocytic tumor initiation is unclear. Sustained expression of *BRAF*<sup>V600E</sup> induces nevus-like growth of melanocytes in transgenic zebrafish<sup>3</sup> and benign growth of epithelial cells in transgenic mice,<sup>4</sup> indicating that *BRAF*<sup>V600E</sup> may induce abnormal cell growth during development. However, introduction of *BRAF*<sup>V600E</sup> into primary human melanocytes induces cell cycle arrest and senescence.<sup>5</sup> A more recent study, conversely, has shown that a minor population of primary human melanocytes may survive sustained expression of *BRAF*<sup>V600E</sup>; however, those observations were not the focus of that particular study.<sup>6</sup>

The p53 protein is a master transcription factor and a key responder to a variety of stresses, including DNA damage, genomic stability, hypoxia, and oncogenic aberrations.<sup>7</sup> TP53 mutations or deletions have been detected in approximately 50% of cancers. However, TP53 mutations in human melanoma are not common, with reports ranging from nearly absent up to 10%<sup>8</sup> and mel-

Supported by Specialized Program of Research Excellence (SPORE) on Skin Cancer (CA-093372) 5R21CA116103 and Melanoma Research Foundation.

H.Y. and R.M. contributed equally to this work.

Accepted for publication March 12, 2009.

Supplemental material for this article can be found on <http://ajp.amjpathol.org>.

Address reprint requests to Xiaowei Xu, M.D., Ph.D., Department of Pathology and Laboratory Medicine, University of Pennsylvania School of Medicine, 3400 Spruce Street, Philadelphia, PA 19104, E-mail: xug@mail.med.upenn.edu; or Meenhard Herlyn, DMV, The Wistar Institute, 3601 Spruce Street, Philadelphia, PA, 19104, E-mail: herlynm@wistar.org.

anomas express normal or augmented levels of p53.<sup>9–11</sup> Since melanomas are resistant to apoptosis,<sup>12</sup> the function of p53 in melanomas is puzzling. Studies in transgenic mice expressing a melanocyte specific activated HRAS allele on a p53-null background provide strong evidence for p53 inactivation during melanoma genesis.<sup>13</sup> More recently, an 'epithelial-like' melanoma subtype was shown to have significantly higher frequency of p53 inactivation.<sup>14</sup> We have shown that melanomas exhibit impaired p53-dependent apoptosis<sup>15</sup> and p53-target genes are often dissociated from p53 regulation,<sup>16</sup> suggesting the p53 pathway is impaired in melanomas. A better understanding of the mechanisms of p53 pathway dysregulation in melanoma will be necessary to understand the molecular steps during transformation and to develop better chemotherapeutic strategies.

Melanomas commonly arise from nevi,<sup>17</sup> suggesting that transformation of melanocytes requires a bypass of the senescent response induced by mutant *BRAF*. Here, we show that sustained expression of *BRAF*<sup>V600E</sup> does not induce oncogene-induced senescence in all infected human melanocytes; rather, a subpopulation of melanocytes survives. The acquisition of an additional insult, namely disruption of p53, immortalizes these cells and promotes an early transformed cell phenotype both *in vitro* and *in vivo*. Loss of p53 function in these cells may also result in genetic instability and loss of retinoblastoma (Rb)1 locus. These data support a tumor suppressor role for p53 in melanoma. Gene expression profiling analyses show clear disparities between p53 target gene expression in melanomas and nevi, suggesting a dysfunctional p53 pathway *in vivo*. Together, these data suggest that the *BRAF*<sup>V600E</sup> mutation is a founder event for melanocytic lesion formation, and disruption of p53 pathway may be critical for melanocyte transformation.

## Materials and Methods

### Plasmids

We used the pBABE plasmid (courtesy of D. Herlyn; The Wistar Institute, Philadelphia, PA) to clone human *BRAF*<sup>V600E</sup> into the pLenti6 lentiviral plasmid (Invitrogen, Carlsbad, CA) and verified sequences by sequencing both strands. The p53 small interfering RNA lentiviral plasmid with green fluorescent protein (GFP) tag was a generous gift from M. Soengas (University of Michigan, Ann Arbor, MI).

### Cell Culture, Retroviral Transduction, Cell Proliferation, and $\beta$ -Galactosidase Activity

Primary human melanocytes were isolated from the epidermis of neonatal foreskin as previously described.<sup>18</sup> The melanocytes were maintained in melanocyte 254CF medium and human melanocyte growth supplement-2 (Cascade Biologics, Portland, OR). Transformed cells were also cultured in Tu 2% medium (MCDB153/L15 medium (v/v: 4/1) supplemented with 2% fetal bovine serum, insulin (5 units/ml), CaCl<sub>2</sub> (2 mmol/L), 100 U/ml

penicillin, and 100 mg/ml streptomycin). Production of pseudotyped lentivirus was achieved as previously described.<sup>19</sup> Lentiviral vectors pLenti6/*BRAF*<sup>V600E</sup>, p53 short hairpin (sh)RNA-GFP, and GFP vector were used to infect melanocytes. *BRAF*<sup>V600E</sup>-infected cells were then selected in 6  $\mu$ g/ml blasticidin-containing melanocyte culture medium. Cultured cells were stained for SA- $\beta$ -galactosidase (SA- $\beta$ -Gal) activity (Promega, Fitchburg, WI).

### Western Blot, Immunocytochemistry, Immunohistochemistry, and Quantitative PCR

Western blots were performed as previously described.<sup>20</sup> The antibodies used for Western blotting were pERK (1:1000; Cell Signaling), p53 (1: 50 Cell Signaling), and  $\beta$ -actin (1:5000; Sigma). Immunohistochemistry and immunocytochemistry were performed as previously described.<sup>21</sup> The antibodies used were anti-S-100 (1:500; Dakocytomation), Melan-A (1:75; Novocasta Lab Ltd), tyrosinase (1:75; Novocasta Lab Ltd), and phosphor-H2AX (1:50; EMD Chemicals). 4,6-Diamidino-2-phenylindole staining was used to visualize nuclei.

### Soft Agar and Matrigel Migration Assays

For soft agar assay, cells (5000 to 10,000 per well) were seeded in 0.5% low-melting-point agarose in Dulbecco's Modified Eagle Medium with 10% fetal bovine serum, layered onto 0.8% agarose in Dulbecco's Modified Eagle Medium/10% fetal bovine serum. Colonies were enumerated and photographed at  $\times 200$  magnification 8 weeks after seeding. The Matrigel *in vitro* migration assay was performed using BD BioCoat Tumor invasion system (BD Biosciences, Franklin Lakes, NJ).

### Human Skin Reconstructs

Human skin reconstructs were generated as described.<sup>21,22</sup> Briefly, dermal reconstructs consisted of bovine collagen type I with embedded dermal fibroblasts. Control or melanocytes infected with various vectors were seeded into tissue reconstruct trays together with keratinocytes onto dermal reconstructs at a 1:5 ratio of melanocytic cells to keratinocytes. Two weeks later, reconstructs were harvested and fixed in 10% neutral buffered formalin for 2 to 3 hours, processed by routine histological methods, embedded in paraffin, and sectioned. After sectioning, the reconstructs were stained with Melan-A or S-100 to depict melanocytes.

### Xenograft Experiments

We injected  $2 \times 10^6$  normal melanocytes or melanocytes with *BRAF*<sup>V600E</sup> and p53 knockdown (*V600E*<sup>+</sup>/*p53*<sup>sh</sup>) subcutaneously into the flanks of non-obese diabetic-severe combined immunodeficiency mice (10 mice each group) in 100  $\mu$ l Matrigel (BD Biosciences, San Jose, CA). After tumors were palpable ( $\sim 2$  weeks), caliper measurements were obtained every 72 hours. Tumor vol-

ume was monitored closely for 9 weeks, at which time the animals were sacrificed. All of the organs were examined for metastasis and preserved. The tumors were excised and processed for histology.

### *Human Tissue Samples and Microarray Study*

Excessive tissues from surgical resection specimens of nevi or melanomas were used in this study. The protocol has been approved by University of Pennsylvania Institutional Review Board. All of the specimens were fresh frozen and stored in  $-80^{\circ}\text{C}$  before use. Total RNA was extracted from homogenized tissues and 10  $\mu\text{g}$  total RNA was used for cDNA Synthesis (Invitrogen, Carlsbad, CA). Labeled cRNA was fragmented and hybridized to the Human Genome U133A Array (Affymetrix, Santa Clara, CA) that contains 14,500 genes. The hybridization and data collection were performed at the University of Pennsylvania microarray core facility.

### *Gene Expression Microarray Data Analysis*

Gene expression data from Affymetrix microarrays from two databases were used. The first dataset<sup>23</sup> was obtained from Gene Expression Omnibus (GSE 3189) that had Affymetrix 133A microarray data available on 63 samples (18 nevi, and 45 melanomas). MAS5.0 was used to derive gene expression values by the original authors. The second dataset included data from Affymetrix microarrays done at University of Pennsylvania microarray facility from 33 samples (14 nevi, 19 melanomas). Robust multichip analysis was used to derive gene expression values.<sup>24</sup>

Genes were included in this analysis if there was expression and sufficient variability across all samples in a dataset. In the first dataset, a gene was excluded when either its mean expression or the range of its expression values (for all samples) was less than 75. In the second dataset, 30 was used instead of 75. Hierarchical cluster analysis using Euclidean distance was used to cluster genes and samples for the heatmaps. A two-sample *t*-test was performed for each probeset, assuming equal or unequal variances as indicated by the test for equal variances. Adjusted *P* values were computed using the Benjamini-Hochberg procedure to adjust for multiple hypothesis tests (results in supplemental Table S1 at <http://ajp.amjpathol.org>). Genespring was used to process the gene expression data and produce the heatmaps. Statistical analyses were done using SAS Version 9.03.

### *Array-Based Comparative Genomic Hybridization*

Array based comparative genomic hybridization (aCGH) was performed onto the platform with  $\sim 5000$  human bacterial artificial chromosomes spaced at an average of 1Mb across the genome developed at the University of Pennsylvania.<sup>25</sup> For hybridization, 1  $\mu\text{g}$  of test DNA and 1  $\mu\text{g}$  of sex-match pooled normal human DNA (obtained

from a set of ten healthy female or male volunteers) were labeled with either Cy3-dCTP or Cy5-dCTP (Amersham Biosciences, UK) incorporated by random priming (Bioprime Labeling Kit, Invitrogen, Carlsbad, CA). Equal amounts of test and reference DNA (1  $\mu\text{g}$  each) were mixed and precipitated with Cot1-DNA, 3M NaOAc (pH 7.0) and ethanol. Arrays were hybridized with 50% deionized formamide, 2 $\times$  SSC, 2% SDS, 10% dextran sulfate, and 100  $\mu\text{g}/\mu\text{l}$  of yeast tRNA for 72 hours at 37 $^{\circ}\text{C}$  in a moist chamber on a slowly rocking table. Slides were washed and arrays were scanned on a GenePix 4000B dual scanner (Axon Instruments, Downingtown, PA).

### *Array-CGH Data Analysis*

Fluorescent data from hybridization images were processed and analyzed with Gene Pix Pro 5.0 (Axon Instruments, Union City, CA) to obtain the  $\log_2$  ratios (tumor/reference) of each slide. Array-CGH data were processed through print-tip loess normalization, using the DNMAD application, which also allowed us to merge and filter clones between replicates in a slide and in the dye-swap experiment. We filtered out inconsistent replicates (those ones with a  $\log_2$  ratio distant to the median  $\log_2$  ratio of the replicates greater than 0.3) and clones that did not have available data in more than 70% of the cases. For visualization and detection of copy number alteration we used "Analysis of Copy number Errors" algorithm in CGH-Explorer (V 3.1b), estimates copy number calls based on genomic regions rather than on individual bacterial artificial chromosomes.  $\log_2$  ratios for each of the bacterial artificial chromosomes are plotted according to chromosome position using a "moving average smoother" with a three-clone window. The significance is expressed by the estimation of the positive false discovery rate; in our case the positive false discovery rate chosen was 0.1.

### *Statistical Analysis*

One-way analysis of variance (analysis of variance), followed by Tukey's multiple comparison test was used to analyze the data comparing groups with different treatments. Statistical significance was determined if the two-sided *P* value of a test was less than 0.05.

## **Results**

### *Generation of BRAF<sup>V600E</sup> Positive Human Melanocytes*

We infected foreskin-derived primary melanocytes with bicistronic lentiviral vectors co-expressing BRAF<sup>V600E</sup> and a blasticidin resistance cassette. During selection in blasticidin-containing medium, most BRAF<sup>V600E</sup>-infected melanocytes ( $\sim 95\%$ ) gradually stopped proliferating and exhibited intense SA- $\beta$ -Gal activity (data not shown) similar to previous studies.<sup>5,26</sup> However, a subpopulation of BRAF<sup>V600E</sup>-positive melanocytes ( $\sim 5\%$  of cells seeded) survived and proliferated in the selection medium. These



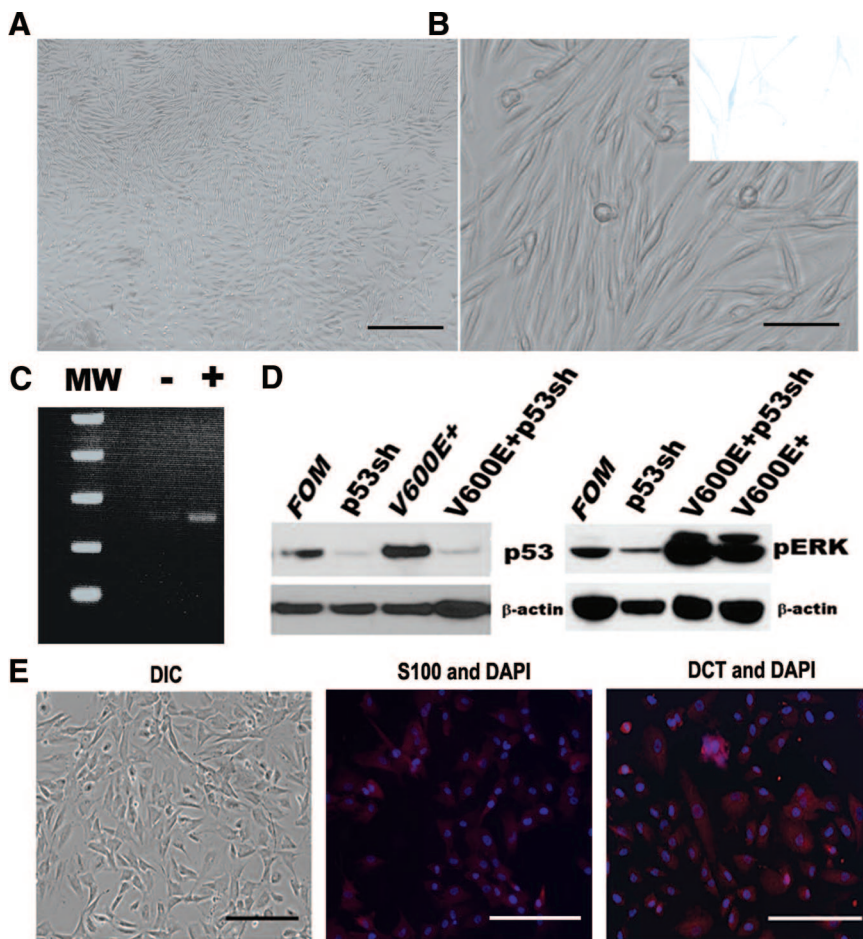


**Figure 1.** Isolation and characterization of V600E<sup>+</sup> primary human melanocytes. *BRAF*<sup>V600E</sup>-infected human melanocytes were selected and expanded in the blasticidin containing medium. **A:** Confluent growth of V600E<sup>+</sup> primary human melanocytes in culture. Scale bar = 100 μm. Representative images from at least nine independent experiments. **B:** V600E<sup>+</sup> melanocytes retained typical melanocyte morphology. Scale bar = 20 μm. **Inset:** V600E<sup>+</sup> melanocytes did not show significant SA-β-Gal activity. **C:** V600E<sup>+</sup> melanocytes expressed *BRAF*<sup>V600E</sup> gene by reverse transcription PCR, while control melanocytes did not express *BRAF*<sup>V600E</sup>. **D:** V600E<sup>+</sup> melanocytes were infected with lentivirus with p53 shRNA (p53<sup>sh</sup>). Western blot analysis for p53 and pERK in control (FOM) and infected cells. The expression of p53 protein was significantly decreased in cells infected with p53 shRNA, while pERK levels were significantly increased after *BRAF*<sup>V600E</sup> infection. The blots represent typical results from three independent experiments. **E:** Representative image of V600E<sup>+</sup>/p53<sup>sh</sup> melanocytes at passage 11. Differential interference contrast showed that cells became more epithelioid with abundant cytoplasm. Scale bar = 40 μm. Cells were stained with antibody against either S-100 or dopachrome tautomerase, and nuclei were visualized with 4,6-diamidino-2-phenylindole. Scale bar = 20 μm.

cells grew to confluence within one month and they retained typical melanocyte morphology (Figure 1A). These cells did not show significant SA-β-Gal activity (Figure 1B, right corner insert). Similar results were obtained from primary melanocytes derived from at least nine different individuals. Normal melanocytes infected with lentivirus carrying GFP were not able to survive in blasticidin selection medium after 2 days of selection (data not shown). Using a primer pair specific for *BRAF*<sup>V600E</sup>, reverse transcription-PCR was performed to verify that these surviving melanocytes expressed the exogenous oncogene product (Figure 1C). These cells had a similar lifespan as normal melanocytes and they can be passaged 10 to 12 times *in vitro*. These data suggest that a subpopulation may respond to *BRAF*<sup>V600E</sup> differently than the overwhelming majority of melanocytes.

#### Knockdown of p53 Increases Proliferation of V600E<sup>+</sup> Melanocytes

p53 function in melanoma is thought to be largely inactive, so we began to examine the role of p53 in melanocytes harboring the *BRAF*<sup>V600E</sup> gene product. To disrupt p53 function in V600E<sup>+</sup> melanocytes, p53 shRNA was expressed from a lentiviral vector co-expressing GFP. Immunoblotting was performed to confirm the knock-

down of p53 protein expression in these cells. As shown in Figure 1D, p53 shRNA effectively decreased the expression of p53 protein in infected cells but had no significant effect on pERK levels; as expected, pERK was heightened in V600E<sup>+</sup> melanocytes. After about 10 passages, V600E<sup>+</sup>/p53<sup>sh</sup> melanocytes acquired an epithelioid cellular morphology, reminiscent of the morphology of melanoma cells in culture (Figure 1E). To ensure that these cells were indeed of melanocytic origin, they were assayed for specific markers; as measured by quantitative reverse transcription PCR, they expressed microphthalmia-associated transcription factor and Tyrp1, suggesting that contaminant cell types were not responsible for the observed phenotype (data not shown). Subsequent immunocytochemical stains demonstrated that they continued to express other melanocytic markers such as dopachrome tautomerase, S-100, and HMB45 (S-100 and dopachrome tautomerase: Figure 1E; HMB45, data not shown).

We compared the growth rate of control, V600E<sup>+</sup>, p53 knockdown (p53<sup>sh</sup>), and V600E<sup>+</sup>/p53<sup>sh</sup> melanocytes in melanocyte growth medium. V600E<sup>+</sup> melanocytes grew slightly slower than control melanocytes in the medium, but the difference was not statistically significant. While p53 knockdown moderately increased melanocyte proliferation rate, V600E<sup>+</sup>/p53<sup>sh</sup> melanocytes displayed dra-

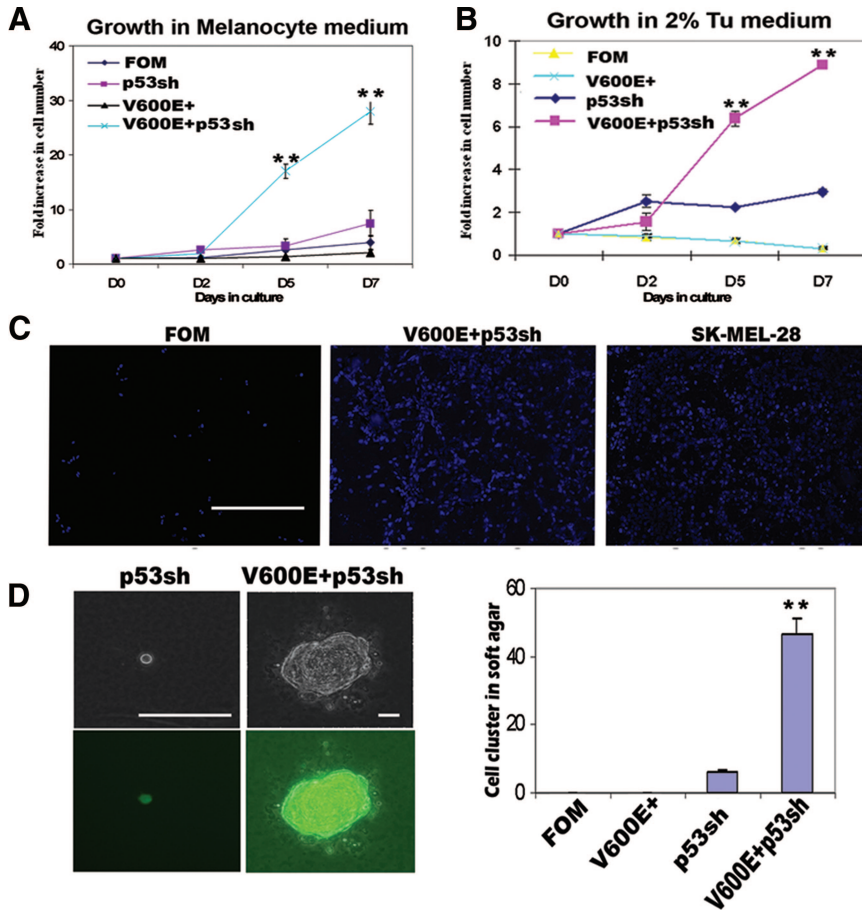


**Figure 2.** V600E<sup>+</sup>/p53<sup>sh</sup> melanocytes show transformed phenotype *in vitro*. **A:** Cells were cultured in the melanocyte growth medium and their growth rates were measured. V600E<sup>+</sup> melanocytes grew slowest, while V600E<sup>+</sup>/p53<sup>sh</sup> melanocytes grew most quickly with a 30-fold increase in cell number by day 7. **B:** Cells were cultured in 2% Tu medium, which does not support growth of normal melanocytes, and their growth rates were measured. Control and V600E<sup>+</sup> melanocytes were not able to grow in this medium. p53<sup>sh</sup> melanocytes were able to proliferate initially but then reached a growth plateau after 2 days. V600E<sup>+</sup>/p53<sup>sh</sup> melanocytes proliferated well in this medium. **C:** Matrigel migration assay. Normal melanocytes and SK-Mel-28 melanoma cells were used as negative and positive controls, respectively. Nuclei of the cells that penetrated the transwell were stained with 4,6-diamidino-2-phenylindole. V600E<sup>+</sup>/p53<sup>sh</sup> melanocytes can migrate efficiently through the transwell similar to melanoma cells. Scale bar = 100 μm. **D:** Soft agar assay. Control or V600E<sup>+</sup> melanocytes were not able to survive in the soft agar. A few single cells or 2- to 3-cell clusters of p53<sup>sh</sup> melanocytes were present in the soft agar after 6 weeks, while V600E<sup>+</sup>/p53<sup>sh</sup> melanocytes were able to proliferate and form large colonies. Since p53 shRNA vectors also contained GFP, these colonies showed green fluorescence. Scale bars = 200 μm. The number of cell clusters in each well were counted and averaged, V600E<sup>+</sup>/p53<sup>sh</sup> melanocytes formed significantly more cell clusters. The experiments were repeated at least three times. \*\**P* < 0.01 compared to control.

matically increased cell growth. Indeed, the V600E<sup>+</sup>/p53<sup>sh</sup> cell number increased 30-fold after 7 days (Figure 2A). These results indicate that p53 knockdown dramatically increases the proliferation capacity of the V600E<sup>+</sup> human melanocytes.

### V600E<sup>+</sup>/p53<sup>sh</sup> Melanocytes Acquire a Transformed Cell Phenotype *in Vitro*

Growth factor-independent proliferation is often associated with malignant transformation.<sup>27</sup> For optimal growth, human melanocytes normally require basic fibroblast growth factor, stem cell factor, or 12-O-tetradecanoyl phorbol 13-acetate.<sup>28</sup> To test whether V600E<sup>+</sup>/p53<sup>sh</sup> melanocytes have acquired growth factor-independence, we cultured these cells in a minimal medium (Tu 2%) that supports the growth of melanoma cells, but not normal melanocytes. While control melanocytes and V600E<sup>+</sup> melanocytes were not able to survive in this medium, p53<sup>sh</sup> melanocytes proliferated for the first 2 days and subsequently reached a growth plateau. In contrast, V600E<sup>+</sup>/p53<sup>sh</sup> melanocytes continued to proliferate indefinitely, suggesting that these cells have acquired the ability to grow in the absence of growth factors that are essential for normal melanocytes (Figure 2B).

Because the morphology of the V600E<sup>+</sup>/p53<sup>sh</sup> melanocytes resembled melanoma cells, we sought to determine whether they also possessed biological properties

often associated with transformed cells. In a Matrigel migration assay, V600E<sup>+</sup>/p53<sup>sh</sup> melanocytes migrated through Matrigel at a similar rate as malignant SK-Mel-28 melanoma cells (Figure 2C). To test whether these cells are capable of anchorage-independent growth, soft agar assays were performed. As expected, control melanocytes and V600E<sup>+</sup> melanocytes did not survive in soft agar. Only single cells or 2 to 3 cell clusters were observed for p53<sup>sh</sup> melanocytes after 6 weeks in soft agar. However, V600E<sup>+</sup>/p53<sup>sh</sup> melanocytes were able to form large and many colonies within 6 weeks (Figure 2D). These results indicate that V600E<sup>+</sup>/p53<sup>sh</sup> melanocytes have acquired a transformed cell phenotype *in vitro*.

### V600E<sup>+</sup>/p53<sup>sh</sup> Melanocytes Acquire Features of *In Situ* Melanoma Cells in Artificial Human Skin Reconstructs

To study the interaction of V600E<sup>+</sup> and V600E<sup>+</sup>/p53<sup>sh</sup> melanocytes with epidermal keratinocytes and dermal fibroblasts, we introduced these melanocytes into artificial human skin reconstructs that mimic human skin architecture.<sup>18</sup> As expected, normal melanocytes migrated to the dermal-epidermal (d-e) junction with non-continuous distribution (Figure 3A, control). V600E<sup>+</sup> melanocytes also migrated to the d-e junction with non-continuous distribution, however, the cell size was increased and



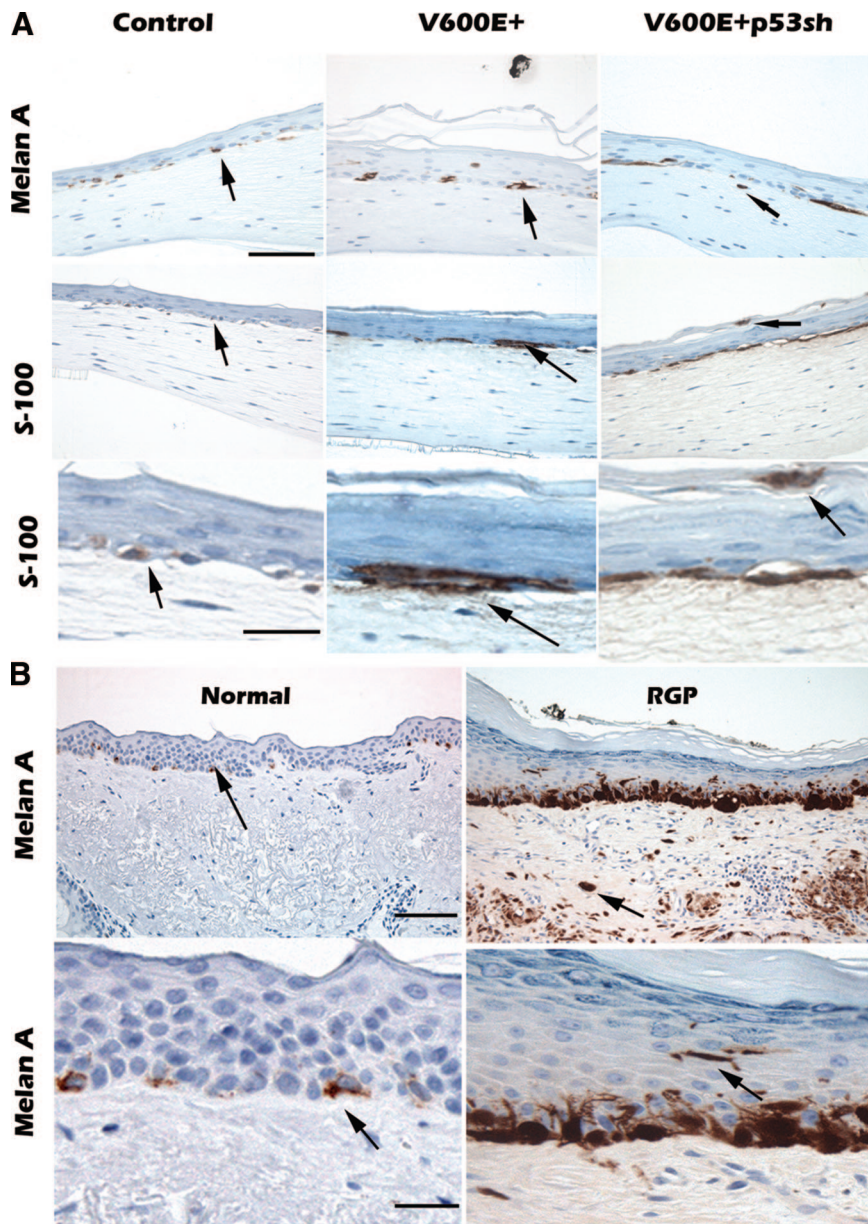


**Figure 3.** V600E<sup>+</sup>/p53<sup>sh</sup> melanocytes form *in situ* melanoma in skin reconstructs. V600E<sup>+</sup>/p53<sup>sh</sup> control, V600E<sup>+</sup> and V600E<sup>+</sup>/p53<sup>sh</sup> were mixed with keratinocytes and laid on top of dermal collagen and fibroblasts. The skin reconstructs were harvested and tissue sections were stained with Melan-A or S-100 to visualize the melanocytes or melanoma cells. **A:** Normal melanocytes migrated to the d-e junction with non-continuous growth pattern in skin reconstructs. **Arrows** point to positive single cells. V600E<sup>+</sup> melanocytes migrated to the d-e junction with non-continuous growth patterns and occasionally formed nests. The cell size was increased compared with normal melanocytes. **Arrows** point to single and nested positive cells. V600E<sup>+</sup> p53<sup>sh</sup> melanocytes migrated to the d-e junction with focal continuous growth pattern and pagetoid proliferation (**arrows**); and rare tumor cells are in the dermis (**arrow**). The experiments were repeated three times. **B:** Normal human skin and radial growth phase melanoma are shown for comparison. In normal human skin, melanocytes are present at the d-e junction with non-continuous growth pattern. **Arrows** point to positive melanocytes. Spontaneous human melanoma *in situ* with microinvasion, melanoma cells are present at the d-e junction with continuous growth pattern, pagetoid proliferation, and invasive tumor cells in the dermis (**arrow**). Scale bars in low power view = 100  $\mu$ m; scale bars in high power view = 20  $\mu$ m.

occasional aggregates of melanocytes were present at the d-e junction; aggregation is a characteristic feature of nevus cells (Figure 3A, V600E<sup>+</sup>). In contrast, V600E<sup>+</sup>/p53<sup>sh</sup> melanocytes demonstrated focal continuous distribution with occasional pagetoid proliferation (Figure 3A, V600E<sup>+</sup>/p53<sup>sh</sup>). In addition, rare cells were observed in the dermis, a morphology that is similar to *in situ* melanoma with microinvasion. Normal melanocytes in human skin tissue show non-continuous distribution at the dermal epidermal junction (d-e junction) (Figure 3B, normal), while *in situ* melanoma often shows continuous distribution of enlarged melanoma cells at the d-e junction with pagetoid proliferation (upward movement of melanocytes to the granular layer of the epidermis) (Figure 3B, radial growth phase). Therefore, V600E<sup>+</sup>/p53<sup>sh</sup> melanocytes have acquired at least some features of radial growth phase melanoma cells, such as continuous proliferation

near the d-e junction, pagetoid proliferation, and increased cell size.

### V600E<sup>+</sup>/p53<sup>sh</sup> Melanocytes Are Weakly Tumorigenic *in Vivo*

To determine whether the transformed melanocytes were tumorigenic *in vivo*,  $2 \times 10^6$  normal or V600E<sup>+</sup>/p53<sup>sh</sup> melanocytes were subcutaneously injected into the flanks of non-obese diabetic-severe combined immunodeficiency mice (10 mice each group). Tumor volume was monitored closely for 9 weeks, at which time the animals were sacrificed, tumors were excised, and tissue was preserved for analysis. As expected, normal melanocytes were not able to form tumors in these mice (Figure 4A, control), but V600E<sup>+</sup>/p53<sup>sh</sup> melanocytes

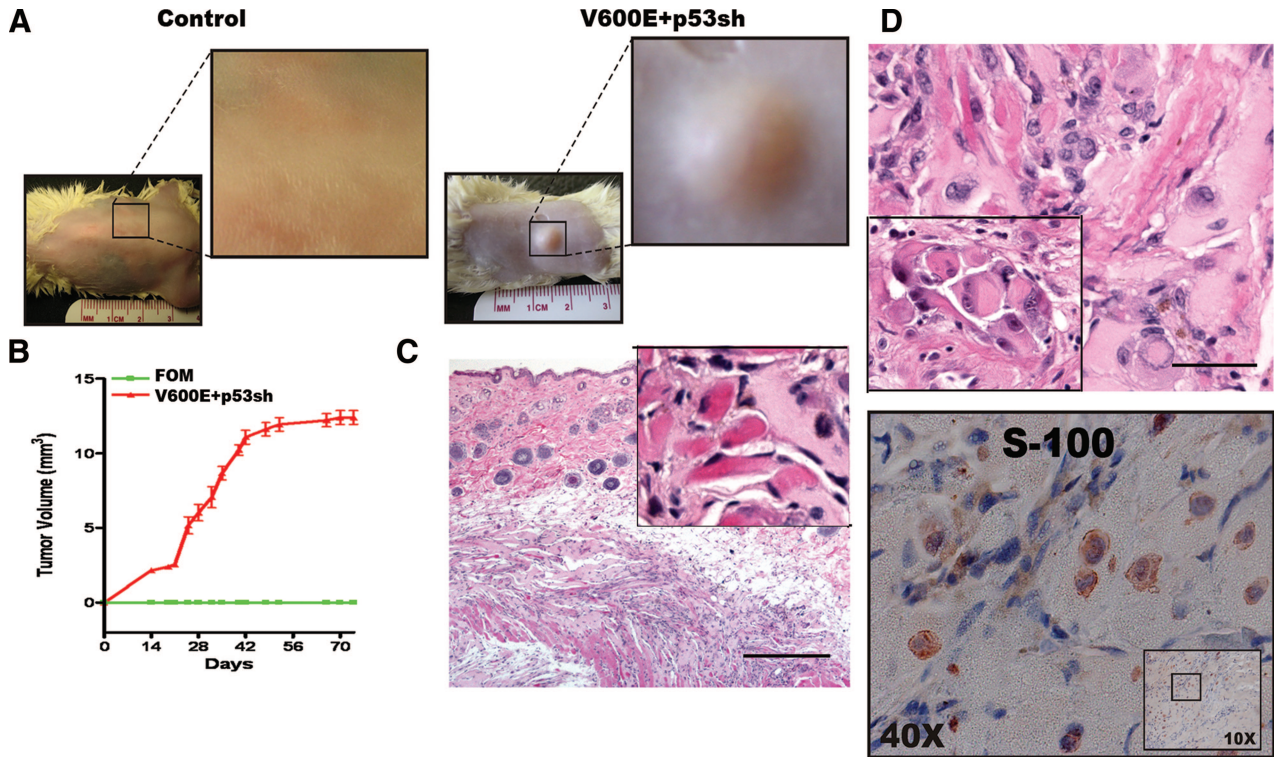


**Figure 4.** V600E<sup>+</sup>/p53<sup>sh</sup> melanocytes are tumorigenic *in vivo*. **A:** Control and V600E<sup>+</sup>/p53<sup>sh</sup> melanocytes were injected subcutaneously into non-obese diabetic-severe combined immunodeficiency mice. Control melanocytes were not able to form tumors. V600E<sup>+</sup>/p53<sup>sh</sup> melanocytes were able to form xenografts in 100% of injected mice (10/10). **B:** Tumor growth curve. The tumors became palpable after 2 weeks and continued to grow for 6 weeks and reach a plateau. **C:** Xenograft-derived tumor cells infiltrated the muscle fibers. **Inset:** tumor cells infiltrating eosinophilic skeletal muscle fibers. **D:** V600E<sup>+</sup>/p53<sup>sh</sup> melanocytes in the xenografts showed severe nuclear atypia and had morphological features of human melanoma cells. **Inset:** histology of human melanoma cells for comparison. V600E<sup>+</sup>/p53<sup>sh</sup> melanocytes within the xenografts were positive for S100 (**below**). Scale bar in **(C)** = 100  $\mu$ m; scale bar in **(D)** = 20  $\mu$ m.

formed palpable masses after 2 weeks in 100% of animals (Figure 4A, V600E<sup>+</sup>/p53<sup>sh</sup>). However, the tumor growth reached a plateau after 6 weeks and these mice were sacrificed shortly thereafter (Figure 4B). Histology of the xenografts showed that tumor cells had infiltrated the muscle (Figure 4C), and these cells had enlarged nuclei and prominent nucleoli, some with nuclear inclusions (Figure 4D). The morphology is similar to that of melanoma cells in tissues (Figure 4D, **inset**). However, evidence of metastatic melanoma was not seen in these mice. The tumor cells were positive for both S-100 (Figure 4D) and tyrosinase (not shown). Immunohistochemical stain of Ki-67 was performed and only rare tumor cells were positive and few blood vessels were present in the xenografts (data not shown). These results indicate that V600E<sup>+</sup>/p53<sup>sh</sup> melanocytes are tumorigenic *in vivo*, but the tumorigenicity is weak and these cells are not yet capable of metastasis.

### *Dysregulation of p53 Pathway during Progression from Nevi to Melanomas*

The expression of normal or high levels of p53 protein in melanoma cells is intriguing, as melanoma cells are highly resistant to apoptosis. Although the exact mechanism is unknown, this paradoxical observation may be explained by dysregulated p53 functionality in mel-

anoma cells. Previous studies have demonstrated that activation of p53 observed in melanoma cell lines does not correlate with the regulation of its target genes, suggesting functional inactivation of p53 in melanomas.<sup>16</sup> To demonstrate alteration in the p53 transcriptional activity during melanocytic tumor progression, we compared p53-target gene expression using gene expression profiling data from two independent studies. The first database included 18 nevi and 45 melanomas, and the second included 14 nevi and 19 melanomas. Because p53-target genes are not discriminate from one tissue to another,<sup>29</sup> we included genes that have been identified as p53-target genes in the literature<sup>30–34</sup> for analysis. This set included 97 Affymetrix probesets (some genes had multiple probesets; see supplemental Table S1 at <http://ajp.amjpathol.org> for the probe sets included for each set). Using these confirmed p53-target genes, we found that a majority of benign nevi can be separated from melanomas (59 of 63 samples were correctly classified) in the first data set. These p53-target genes were able to completely stratify nevi from melanomas in the second data set (Figure 5). These data demonstrate that there are indeed alterations in the p53-target gene expression during the progression from nevi to melanomas and suggest that, despite a lack of genetic mutations, the p53 pathway becomes dysfunctional in malignant melanoma.



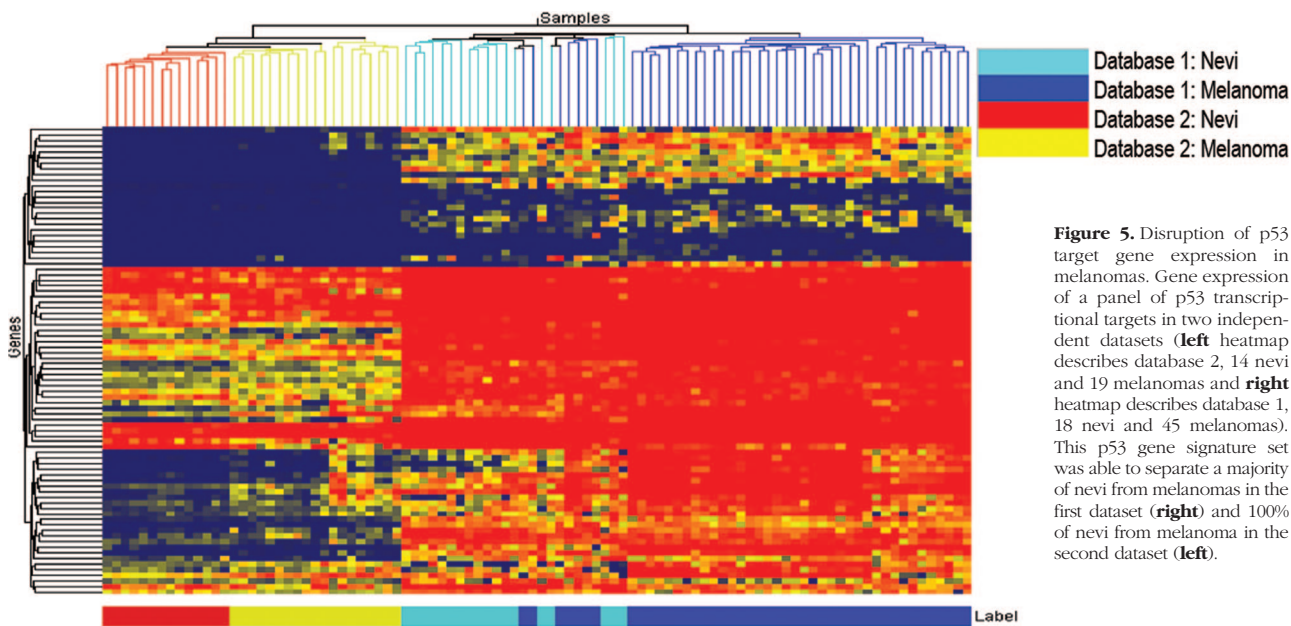


**Figure 5.** Disruption of p53 target gene expression in melanomas. Gene expression of a panel of p53 transcriptional targets in two independent datasets (**left** heatmap describes database 2, 14 nevi and 19 melanomas and **right** heatmap describes database 1, 18 nevi and 45 melanomas). This p53 gene signature set was able to separate a majority of nevi from melanomas in the first dataset (**right**) and 100% of nevi from melanoma in the second dataset (**left**).

### Genomic Instability and Inactivation of Rb Pathway in Transformed V600E<sup>+</sup>/p53<sup>sh</sup> Melanocytes

Inactivation of p53 is known to induce genomic instability.<sup>35</sup> H2AX, a variant form of histone H2A, is phosphorylated on a serine four residues from the carboxyl terminus in response to the introduction of DNA double-strand breaks,<sup>36</sup> and high endogenous levels of phosphorylated H2AX are a consequence of chromatin instability.<sup>37</sup> To examine whether p53 knockdown in melanocytes induces genomic instability, we studied H2AX phosphorylation in V600E<sup>+</sup>/p53<sup>sh</sup> melanocytes and showed that over 50% of cells are highly-positive for phospho-H2AX, as opposed to less than 10% for control melanocytes, indicating genomic instability in these cells (Figure 6A). We then performed aCGH on the transformed cells and compared genome-wide abnormalities to control melanocytes. Representative whole-genome DNA copy number profile for V600E<sup>+</sup>/p53<sup>sh</sup> and parental control melanocytes are shown in Figure 6B. A major genomic deletion in chromosome 13p14, where the tumor suppressor gene *Rb1* is located, was observed in V600E<sup>+</sup>/p53<sup>sh</sup> melanocytes. Although the exact mechanism underlying the deletion is unclear, these data suggest that mutant BRAF and p53 inactivation significantly increase genetic instability and subsequent genetic amplifications/deletions may occur to contribute to the transformation of V600E<sup>+</sup>/p53<sup>sh</sup> melanocytes, in this case, loss of the *Rb1* locus.

### Discussion

In this study, we present surprising findings that a subpopulation of primary human melanocytes can survive mutant BRAF-induced senescence and that those cells acquire early transformed cell phenotypes after disrup-

tion of the p53 pathway. The transformed melanocytes are weakly tumorigenic *in vivo*, and they are not capable of metastasis. This is, to our knowledge, the first report detailing a strategy for transforming human primary melanocytes without the use of human telomerase reverse transcriptase or SV40, often used to immortalize primary cells; these data provide a biological foundation to help elucidate the roles of the MAPK and p53 pathway in the

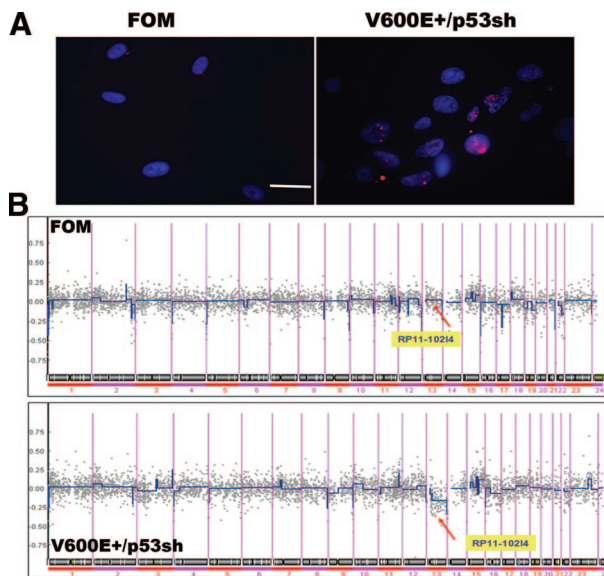


**Figure 6.** Genomic instability and disruption of *Rb1* locus during V600E<sup>+</sup>/p53<sup>sh</sup> melanocyte transformation. **A:** Control and V600E<sup>+</sup>/p53<sup>sh</sup> melanocytes were stained an antibody against phosphorylated H2AX, and nuclei were visualized with 4,6-diamidino-2-phenylindole. Scale bar = 10  $\mu$ m. There is significantly increased H2AX phosphorylation in V600E<sup>+</sup>/p53<sup>sh</sup> melanocytes. **B:** Representative whole-genome DNA copy number profile for V600E<sup>+</sup>/p53<sup>sh</sup> melanocytes and control FOM melanocytes. Log<sub>2</sub> ratios for each of the bacterial artificial chromosomes are plotted according to chromosome position using a “moving average smoother” with a three-clone window. A substantial deletion in chromosome 13p14, where *Rb1* is located, is shown in the V600E<sup>+</sup>/p53<sup>sh</sup> melanocytes, but not parental control cells (arrows point to the described mutations).



etiology of melanoma without artificial factors, such as SV40.

We have previously shown that a combination of growth factors and UV radiation can transform human melanocytes *in vivo*.<sup>18,22</sup> Others have demonstrated that human melanocytes can be fully transformed to melanoma cells without UV radiation using a combination of SV40, human telomerase reverse transcriptase, and Ras or C-Met; a separate study detailed the use of human telomerase reverse transcriptase, p53, the Rb pathway, and Ras or phosphoinositide-3 kinase.<sup>38,39</sup> The results presented here are supported by these earlier studies because activation of the MAPK pathway and inhibition of p53 are central features of each of these studies, albeit through varying methods (SV40 or dominant-negative mutants against p53). However, unlike the previous studies, the transformed V600E<sup>+</sup>/p53<sup>sh</sup> melanocytes are weakly tumorigenic and the tumor growth reaches a plateau after 6 weeks. Transgene down-regulation *in vivo* has been well documented,<sup>40</sup> hence we hypothesize that the cessation of tumor growth is at least partially due to down-regulation of V600E<sup>+</sup> transgene in the xenografts. Nevertheless, additional genetic alterations are likely needed for these cells to become fully metastatic *in vivo*.

It is intriguing to speculate about the differences between the subpopulation of melanocytes that are more susceptible to transformation and those cells that enter oncogene-induced senescence. Our results are in agreement with a recent study by Green and colleagues in which approximately 5% of melanocytes remained alive and retained bromodeoxyuridine labeling after BRAF<sup>V600E</sup> infection; however, their study did not focus on these surviving cells.<sup>6</sup> The possibility exists that this subpopulation is comprised primarily of melanocyte precursor cells, which are more resistant to oncogene-induced senescence. The surviving cells expressed heightened levels of nestin (data not shown), a type VI intermediate filament protein, which is often expressed by neural stem/progenitor cells.<sup>41</sup> We have previously shown that nestin-positive hair bulge neural crest stem cells can be differentiated to melanocytes.<sup>21</sup> Since melanocytes are neural crest-derived, we cautiously postulate that primary human foreskin melanocytes contain a subpopulation of progenitor cells and, unlike mature melanocytes, they are less susceptible to mutant BRAF-induced senescence. However, this remains speculative and only prospective isolation of these progenitor cells may allow us to test this hypothesis.

Melanomas often arise from pre-existing nevi,<sup>17</sup> suggesting that cell cycle arrest in nevi may be overcome by additional genetic or epigenetic changes. The possibility that loss of p53 function is involved in promoting melanoma from a benign nevus is plausible. Indeed, transgenic animal models have demonstrated that growth arrest in BRAF<sup>V600E</sup>-induced benign melanocytic or epithelial tumors can be overcome through concomitant mutation of TP53.<sup>3,4</sup> p53 inactivation can cooperate with activated RAS to promote the development of cutaneous melanomas that are clinically indistinguishable from those arisen on the INK4a(Delta2/3) null background.<sup>13</sup> Thus, disruption of the p53 pathway promotes a detour of BRAF<sup>V600E</sup>-induced se-

nescence during tumor development. Related studies have shown that activation of MEK permanently arrests primary murine fibroblasts, but enhances mitogenesis and transformation in cells also lacking p53.<sup>42</sup> Still other studies contradict these data by showing that loss of TP53 does not enable escape from oncogene-induced senescence in human fibroblasts.<sup>43,44</sup> However, these studies used alternative oncogenes and did not involve primary human melanocytes. Weinberg and his colleagues have shown that expression of melanocyte-specific factors present before neoplastic transformation play a pivotal role in governing the outcome of melanocytes after oncogenic insult<sup>38</sup> and, recently, it has been noted that TP53 is indeed one of several genes that are required for bypass of BRAF<sup>V600E</sup>-mediated senescence in human melanocytes.<sup>6</sup> Thus, the role of p53 during oncogene-induced senescence appears to be both species- and cell type-specific, and functional p53 appears to be critical for BRAF<sup>V600E</sup>-induced senescence in human melanocytes.

p53 has a central role in skin pigmentation, and may impact on melanoma initiation and progression; however, the role of p53 in melanoma has been somewhat underappreciated due to its low mutation frequency.<sup>8</sup> The function of p53 in melanoma may be dysregulated by a myriad of mechanisms, including dysregulation of its target genes such as APAF-1<sup>45</sup> and p53-up-regulated modulator of apoptosis.<sup>46</sup> Using two independent gene expression profiling data sets of human melanocytic lesions, we showed that there are indeed alterations in p53-target gene expression during progression from nevi to melanomas. The results support a dysfunctional p53 pathway in melanoma *in vivo*.

Inactivation of p53 increased endogenous H2AX phosphorylation and genomic instability in V600E<sup>+</sup>/p53<sup>sh</sup> melanocytes. The transformed phenotype of V600E<sup>+</sup>/p53<sup>sh</sup> melanocytes appears to result from concomitant deletion in a key locus on chromosome 13 that encodes the *Rb1* gene. This genomic aberration is likely a consequence of genetic instability incurred through increased stress at DNA replication forks via BRAF<sup>V600E</sup> overexpression<sup>47-50</sup> and the lack of p53 to inhibit cell cycle progression and initiate apoptosis. Acquisition of this genomic deletion may affect the p16/Rb pathway in such a manner that cyclin D1 and CDK4 are able to drive cell cycle progression without entering the G1 restriction point.<sup>35</sup> Inactivation of Rb and p53 pathways in melanoma is frequently achieved through genetic loss of the CDKN2A locus.<sup>51</sup> Analyses of three critical human melanoma loci—*CDKN2A*, *TP53*, and *CDK4*—have shown that nearly 80% of melanoma cell lines harbor genetic evidence of impaired Rb and p53 pathway functionality.<sup>52</sup> The observation that interference with both Rb and p53 pathway function is oncogenic in the context of disruption of the BRAF pathway is intriguing and allows for speculation regarding novel drug formulations that may target these pathways for therapeutic benefit in melanoma.

Therefore, our data suggest that the BRAF<sup>V600E</sup> mutation is a founder event in melanocytic neoplasia and inactivation of both p53 and Rb pathways in a subpopulation of human melanocytes harboring BRAF<sup>V600E</sup> appears sufficient to transform these cells. The interaction

between the mutant BRAF and dysfunctional p53 pathway may represent an important mechanism underpinning the genesis of melanoma. Additional biomechanistic studies are currently underway to further delineate the interaction of mutant BRAF and p53 pathways in our system and those results will surely help elucidate the roles of these signaling cascades in melanoma genesis.

## Acknowledgments

We thank Drs. Dorothy Herlyn and Maria Soengas for providing DNA constructs and Dr. J. Li for suggestions on the manuscript.

## References

1. Pollock PM, Harper UL, Hansen KS, Yudt LM, Stark M, Robbins CM, Moses TY, Hostetter G, Wagner U, Kakareka J, Salem G, Pohida T, Heenan P, Duray P, Kallioniemi O, Hayward NK, Trent JM, Meltzer PS: High frequency of BRAF mutations in nevi. *Nat Genet* 2003, 33:19–20
2. Davies H, Bignell GR, Cox C, Stephens P, Edkins S, Clegg S, Teague J, Woffendin H, Garnett MJ, Bottomley W, Davis N, Dicks E, Ewing R, Floyd Y, Gray K, Hall S, Hawes R, Hughes J, Kosmidou V, Menzies A, Mould C, Parker A, Stevens C, Watt S, Hooper S, Wilson R, Jayatilake H, Gusterson BA, Cooper C, Shipley J, Hargrave D, Pritchard-Jones K, Maitland N, Chenevix-Trench G, Riggins GJ, Bigner DD, Palmieri G, Cossu A, Flanagan A, Nicholson A, Ho JW, Leung SY, Yuen ST, Weber BL, Seigler HF, Darrow TL, Paterson H, Marais R, Marshall CJ, Wooster R, Stratton MR, Futreal PA: Mutations of the BRAF gene in human cancer. *Nature* 2002, 417:949–954
3. Patton EE, Widlund HR, Kutok JL, Kopani KR, Amatruda JF, Murphey RD, Berghmans S, Mayhall EA, Traver D, Fletcher CD, Aster JC, Granter SR, Look AT, Lee C, Fisher DE, Zon LI: BRAF mutations are sufficient to promote nevi formation and cooperate with p53 in the genesis of melanoma. *Curr Biol* 2005, 15:249–254
4. Dankort D, Filenova E, Collado M, Serrano M, Jones K, McMahon M: A new mouse model to explore the initiation, progression, and therapy of BRAFV600E-induced lung tumors. *Genes Dev* 2007, 21:379–384
5. Michaloglou C, Vredeveld LC, Soengas MS, Denoyelle C, Kuilman T, van der Horst CM, Majoor DM, Shay JW, Mooi WJ, Peeper DS: BRAFE600-associated senescence-like cell cycle arrest of human naevi. *Nature* 2005, 436:720–724
6. Wajapeyee N, Serra RW, Zhu X, Mahalingam M, Green MR: Oncogenic BRAF induces senescence and apoptosis through pathways mediated by the secreted protein IGFBP7. *Cell* 2008, 132:363–374
7. Sherr CJ: Principles of tumor suppression. *Cell* 2004, 116:235–246
8. Box NF, Terzian T: The role of p53 in pigmentation, tanning and melanoma. *Pigment Cell Melanoma Res* 2008, 21:525–533
9. Hartmann A, Blaszyk H, Cunningham JS, McGovern RM, Schroeder JS, Helander SD, Pittelkow MR, Sommer SS, Kovach JS: Overexpression and mutations of p53 in metastatic malignant melanomas. *Int J Cancer* 1996, 67:313–317
10. Weiss J, Schwechheimer K, Cavenee WK, Herlyn M, Arden KC: Mutation and expression of the p53 gene in malignant melanoma cell lines. *Int J Cancer* 1993, 54:693–699
11. Sparrow LE, Soong R, Dawkins HJ, Iacopetta BJ, Heenan PJ: p53 gene mutation and expression in naevi and melanomas. *Melanoma Res* 1995, 5:93–100
12. Perlis C, Herlyn M: Recent advances in melanoma biology. *Oncologist* 2004, 9:182–187
13. Bardeesy N, Bastian BC, Hezel A, Pinkel D, Depinho RA, Chin L: Dual inactivation of RB and p53 pathways in RAS-induced melanomas. *Mol Cell Biol* 2001, 21:2144–2153
14. Shields JM, Thomas NE, Cregger M, Berger AJ, Leslie M, Torrice C, Hao H, Penland S, Arbiser J, Scott G, Zhou T, Bar-Eli M, Bear JE, Der CJ, Kaufmann WK, Rimm DL, Sharpless NE: Lack of extracellular signal-regulated kinase mitogen-activated protein kinase signaling shows a new type of melanoma. *Cancer Res* 2007, 67:1502–1512
15. Smalley KS, Contractor R, Haass NK, Kulp AN, Tilla-Gokcumen GE, Williams DS, Bregman H, Flaherty KT, Soengas MS, Meggers E, Herlyn M: An organometallic protein kinase inhibitor pharmacologically activates p53 and induces apoptosis in human melanoma cells. *Cancer Res* 2007, 67:209–217
16. Haapajarvi T, Pitkanen K, Laiho M: Human melanoma cell line UV responses show independency of p53 function. *Cell Growth Differ* 1999, 10:163–171
17. Bevona C, Goggins W, Quinn T, Fullerton J, Tsao H: Cutaneous melanomas associated with nevi. *Arch Dermatol* 2003, 139:1620–1624
18. Berking C, Takemoto R, Satyamoorthy K, Shirakawa T, Eskandarpour M, Hansson J, VanBelle PA, Elder DE, Herlyn M: Induction of melanoma phenotypes in human skin by growth factors and ultraviolet B. *Cancer Res* 2004, 64:807–811
19. Balint K, Xiao M, Pinnix CC, Soma A, Veres I, Juhasz I, Brown EJ, Capobianco AJ, Herlyn M, Liu ZJ: Activation of Notch1 signaling is required for beta-catenin-mediated human primary melanoma progression. *J Clin Invest* 2005, 115:3166–3176
20. Kumar SM, Yu H, Edwards R, Chen L, Kazianis S, Brafford P, Acs G, Herlyn M, Xu X: Mutant V600E BRAF increases hypoxia inducible factor-1alpha expression in melanoma. *Cancer Res* 2007, 67:3177–3184
21. Yu H, Fang D, Kumar SM, Li L, Nguyen TK, Acs G, Herlyn M, Xu X: Isolation of a novel population of multipotent adult stem cells from human hair follicles. *Am J Pathol* 2006, 168:1879–1888
22. Berking C, Takemoto R, Satyamoorthy K, Elenitsas R, Herlyn M: Basic fibroblast growth factor and ultraviolet B transform melanocytes in human skin. *Am J Pathol* 2001, 158:943–953
23. Talantov D, Mazumder A, Yu JX, Briggs T, Jiang Y, Backus J, Atkins D, Wang Y: Novel genes associated with malignant melanoma but not benign melanocytic lesions. *Clin Cancer Res* 2005, 11:7234–7242
24. Irizarry RA, Bolstad BM, Collin F, Cope LM, Hobbs B, Speed TP: Summaries of Affymetrix GeneChip probe level data. *Nucleic Acids Res* 2003, 31:e15
25. Greshock J, Naylor TL, Margolin A, Diskin S, Cleaver SH, Futreal PA, deJong PJ, Zhao S, Liebman M, Weber BL: 1-Mb resolution array-based comparative genomic hybridization using a BAC clone set optimized for cancer gene analysis. *Genome Res* 2004, 14:179–187
26. Gray-Schopfer VC, Cheong SC, Chong H, Chow J, Moss T, Abdel-Malek ZA, Marais R, Wynford-Thomas D, Bennett DC: Cellular senescence in naevi and immortalisation in melanoma: a role for p16? *Br J Cancer* 2006, 95:496–505
27. Wossning T, Herzog S, Kohler F, Meixlsperger S, Kulathu Y, Mittler G, Abe A, Fuchs U, Borkhardt A, Jumaa H: Deregulated Syk inhibits differentiation and induces growth factor-independent proliferation of pre-B cells. *J Exp Med* 2006, 203:2829–2840
28. Lee AY, Kim NH, Choi WI, Youm YH: Less keratinocyte-derived factors related to more keratinocyte apoptosis in depigmented than normally pigmented suction-blistered epidermis may cause passive melanocyte death in vitiligo. *J Invest Dermatol* 2005, 124:976–983
29. Riley T, Sontag E, Chen P, Levine A: Transcriptional control of human p53-regulated genes. *Nat Rev Mol Cell Biol* 2008, 9:402–412
30. Sax JK, El-Deiry WS: p53 downstream targets and chemosensitivity. *Cell Death Differ* 2003, 10:413–417
31. Rozan LM, El-Deiry WS: p53 downstream target genes and tumor suppression: a classical view in evolution. *Cell Death Differ* 2007, 14:3–9
32. Laptenko O, Prives C: Transcriptional regulation by p53: one protein, many possibilities. *Cell Death Differ* 2006, 13:951–961
33. Cheah PL, Looi LM: p53: an overview of over two decades of study. *Malays J Pathol* 2001, 23:9–16
34. Yu J, Zhang L: The transcriptional targets of p53 in apoptosis control. *Biochem Biophys Res Commun* 2005, 331:851–858
35. Sherr CJ, McCormick F: The RB and p53 pathways in cancer. *Cancer Cell* 2002, 2:103–112
36. Redon C, Pilch D, Rogakou E, Sedelnikova O, Newrock K, Bonner W: Histone H2A variants H2AX and H2AZ. *Curr Opin Genet Dev* 2002, 12:162–169
37. Yu T, MacPhail SH, Banath JP, Klovov D, Olive PL: Endogenous expression of phosphorylated histone H2AX in tumors in relation to DNA double-strand breaks and genomic instability. *DNA Repair (Amst)* 2006, 5:935–946
38. Gupta PB, Kuperwasser C, Brunet JP, Ramaswamy S, Kuo WL, Gray JW, Naber SP, Weinberg RA: The melanocyte differentiation program predisposes to metastasis after neoplastic transformation. *Nat Genet* 2005, 37:1047–1054

39. Chudnovsky Y, Adams AE, Robbins PB, Lin Q, Khavari PA: Use of human tissue to assess the oncogenic activity of melanoma-associated mutations. *Nat Genet* 2005, 37:745–749
40. Johansen J, Rosenblad C, Andsberg K, Moller A, Lundberg C, Bjorlund A, Johansen TE: Evaluation of Tet-on system to avoid transgene down-regulation in ex vivo gene transfer to the CNS. *Gene Ther* 2002, 9:1291–1301
41. Gilyarov AV: Nestin in central nervous system cells. *Neurosci Behav Physiol* 2008, 38:165–169
42. Lin AW, Barradas M, Stone JC, van AL, Serrano M, Lowe SW: Premature senescence involving p53 and p16 is activated in response to constitutive MEK/MAPK mitogenic signaling. *Genes Dev* 1998, 12:3008–3019
43. Serrano M, Lin AW, McCurrach ME, Beach D, Lowe SW: Oncogenic ras provokes premature cell senescence associated with accumulation of p53 and p16INK4a. *Cell* 1997, 88:593–602
44. Zhu J, Woods D, McMahon M, Bishop JM: Senescence of human fibroblasts induced by oncogenic Raf. *Genes Dev* 1998, 12:2997–3007
45. Soengas MS, Capodiceci P, Polsky D, Mora J, Esteller M, Opitz-Araya X, McCombie R, Herman JG, Gerald WL, Lazebnik YA, Cordon-Cardo C, Lowe SW: Inactivation of the apoptosis effector Apaf-1 in malignant melanoma. *Nature* 2001, 409:207–211
46. Hussein MR, Haemel AK, Wood GS: Apoptosis and melanoma: molecular mechanisms. *J Pathol* 2003, 199:275–288
47. Di Micco R, Fumagalli M, Cicalese A, Piccinin S, Gasparini P, Luise C, Schurra C, Garre' M, Nuciforo PG, Bensimon A, Maestro R, Pelicci PG, d'Adda di Fagagna F: Oncogene-induced senescence is a DNA damage response triggered by DNA hyper-replication. *Nature* 2006, 444: 638–642
48. Bartkova J, Rezaei N, Liontos M, Karakaidos P, Kletsas D, Issaeva N, Vassiliou LV, Kolettas E, Niforou K, Zoumpourlis VC, Takaoka M, Nakagawa H, Tort F, Fugger K, Johansson F, Sehested M, Andersen CL, Dyrskjot L, Orntoft T, Lukas J, Kittas C, Helleday T, Halazonetis TD, Bartek J, Gorgoulis VG: Oncogene-induced senescence is part of the tumorigenesis barrier imposed by DNA damage checkpoints. *Nature* 2006, 444:633–637
49. Mallette FA, Gaumont-Leclerc MF, Ferbeyre G: The DNA damage signaling pathway is a critical mediator of oncogene-induced senescence. *Genes Dev* 2007, 21:43–48
50. Mitsutake N, Knauf JA, Mitsutake S, Mesa C Jr, Zhang L, Fagin JA: Conditional BRAFV600E expression induces DNA synthesis, apoptosis, dedifferentiation, and chromosomal instability in thyroid PCCL3 cells. *Cancer Res* 2005, 65:2465–2473
51. Sharpless NE, Kannan K, Xu J, Bosenberg MW, Chin L: Both products of the mouse Ink4a/Arf locus suppress melanoma formation in vivo. *Oncogene* 2003, 22:5055–5059
52. Yang G, Rajadurai A, Tsao H: Recurrent patterns of dual RB and p53 pathway inactivation in melanoma. *J Invest Dermatol* 2005, 125:1242–1251